Am J Clin Exp Urol 2025;13(2):69-91
www.ajceu.us /ISSN:2330-1910/AJCEU0162712

Review Article

Integration of magnetic resonance imaging and deep learning for prostate cancer detection: a systematic review

Deepak Kumar[1,2,5], Priyank Yadav[2], Kavindra Nath[3], Adree Khondker[4], Uday Pratap Singh[2], Hira Lal[5], Ashish Gupta[1]

[1]Centre of Biomedical Research, Sanjay Gandhi Post Graduate Institute of Medical Sciences Campus, Rae Bareli Road, Lucknow 226014, U.P., India; [2]Department of Urology, Sanjay Gandhi Post Graduate Institute of Medical Sciences, Rae Bareli Road, Lucknow 226014, U.P., India; [3]Department of Radiology, University of Pennsylvania, Philadelphia, PA 19104, USA; [4]Division of Urology, Department of Surgery, University of Toronto, Toronto, ON, Canada; [5]Department of Radiodiagnosis, Sanjay Gandhi Post Graduate Institute of Medical Sciences, Rae Bareli Road, Lucknow 226014, U.P., India

Received December 16, 2024; Accepted March 10, 2025; Epub April 25, 2025; Published April 30, 2025

Abstract: Objectives: This study aims to evaluate the overall impact of incorporating deep learning (DL) with magnetic resonance imaging (MRI) for improving diagnostic performance in the detection and stratification of prostate cancer (PC). Methods: A systematic search was conducted in the PubMed database to identify relevant studies. The QUADAS-2 tool was employed to assess the scientific quality, risk of bias, and applicability of primary diagnostic accuracy studies. Additionally, adherence to the Checklist for Artificial Intelligence in Medical Imaging (CLAIM) guidelines was evaluated to determine the extent of heterogeneity among the included studies. The systematic review followed the Preferred Reporting Items for Systematic Reviews and Meta-Analysis (PRISMA) guidelines. Results: A total of 29 articles involving 17,954 participants were included in the study. The median agreement to the 42 CLAIM checklist items across studies was 61.90% (IQR: 57.14-66.67, range: 40.48-80.95). Most studies utilized T2-weighted imaging (T2WI) and/or apparent diffusion coefficient (ADC) derived from diffusion-weighted imaging (DWI) as input for evaluating the performance of DL-based architectures. Notably, the detection and stratification of PC in the transition zone was the least explored area. Conclusions: DL demonstrates significant advancements in the rapid, sensitive, specific, and robust detection and stratification of PC. Promising applications include enhancing the quality of DWI, developing advanced DL models, and designing innovative nomograms or diagnostic tools to improve clinical decision-making.

Keywords: Deep learning, prostate cancer, multiparametric-MRI, convoluted neural network

Introduction

Despite the advancements in various approaches for prostate cancer (PC) assessment and therapeutic interventions, PC remains a significant health concern among men. As of 2020, PC was the second most frequently diagnosed cancer in men and the fifth leading cause of cancer-related mortality worldwide [1]. The incidence rates vary substantially between transitioned and transitioning countries, with rates of 37.5 and 11.3 per 1,00,000, respectively. However, mortality rates exhibit less variation, recorded at 8.1 and 5.9 per 1,00,000 respectively [1]. Notably, PC is the most frequently diagnosed cancer in more than half of the countries worldwide [1]. In the United States alone, projections for 2023 estimated incidence of 2,88,300 new PC cases and 34,700 PC-related deaths [2].

One of the primary challenges in PC management is the absence of an early and definitive detection modality. Early detection of PC, particularly at the localized stage, enables effective management and substantially improves survival rates. The current detection protocol for PC follows a multimodal approach, incorporating digital rectal examinations (DRE) [3], serum prostate-specific antigen (PSA) level [4], Trans-Rectal Ultrasound (TRUS) [5], multi-parametric-magnetic resonance imaging (mpMRI)

https://doi.org/10.62347/CSIJ8326

Table 1. Limitations of current prostate cancer detection modalities

Sr. No.	Detection modality	Limitations
1	DRE	Crude approach, Not specific for prostate cancer, Subjective test [9], Inter-examiner variability [10], False positivity [17]
2	Serum PSA	False positivity [11], false negativity [11], Higher probability of false positivity associated with factors; Alcohol intake, Age, urinary tract infection [11]. Lower probability of false positivity associated with Diabetes mellitus type II [11]
3	TRUS prostate	Poor accuracy in local staging [5], Fails to stratify the gradings of the PC
4	Mp-MRI prostate	Inter-observer variability [15, 16], Intra-observer variability [16], False negativity [13, 14] and False positivity [13], Very subtle visual differences among benign tissue, indolent cancer and aggressive cancer leads to challenging interpretation [12]. Difficult to evaluate cancer in central gland, Not suitable for patients having low eGFR (<30) for contrast-based studies, claustrophobic nature, metallic implant in the imaging field. Time consuming tactic
5	Prostate TRUS-biopsy	Blind to the location of the prostate [13], over-diagnosis of clinically insignificant prostate cancer [13], under-diagnosis of clinically significant prostate cancer [13], including the condition if tumor is small, present at restricted zone to approach by biopsy needle. Post-TRUS biopsy complications [5] e.g. Haematospermia, bleeding from urethra, urinary bladder, fever, urosepsis, rectal bleeding, prostatitis, epididymitis, urine retention, etc.

[6], TRUS biopsy [7] and TRUS/MRI-guided fusion biopsy [8], However, each of these modalities presents inherent limitations [5, 9-17] (**Table 1**).

A meta-analysis of pooled data sets has reported sensitivity and specificity values for different modalities: DRE (51% and 59%) [17] PSA (93%, and 20%) [18] TRUS-biopsy (48% and 96%) [13] and mpMRI (93% and 41%) [13]. Additionally, for detecting extracapsular extension (T3 disease), TRUS sensitivity and specificity range from 50% to 92% and 46% to 91%, respectively [5].

MRI has emerged as a promising non-invasive and non-ionizing imaging technique for PC diagnostics. mpMRI integrates anatomical imaging, such as T2 weighted imaging (T2WI), with functional MRI techniques, including diffusion-weighted imaging (DWI), DWI derived apparent diffusion coefficient (ADC) mapping, and dynamic contrast enhanced (DCE) imaging. MpMRI plays a crucial role in PC risk stratification by reducing, unnecessary biopsies and minimizing overtreatment [19, 20].

This imaging techniques has demonstrated sensitivity and specificity rates exceeding 80%, particularly when utilizing a combination of anatomical and functional imaging sequences. Notably, DWI outperforms T2WI alone in sensitivity, area under the receiver operating characteristics (AUROC), and specificity [21].

The Prostate Imaging Reporting and Data System (PI-RADS) serves as a standardized framework for lesion evaluation based on structured scoring criteria [19, 22-24]. PI-RADS outlines the minimal technical requirements for prostate mpMRI acquisition and the Prostate imaging quality (PI-QUAL) scoring system has been introduced to enhance diagnostic accuracy [25]. PI-RADS version 2.1 includes refinements for scoring ambiguous lesions, particularly in the transition zone (TZ) on T2WI and update lesion assessment using DWI [26]. However, despite these improvements, PIRADS exhibits inter- and intra-observer variability, necessitating a high level of expertise for accurate assessment [15, 16] (**Table 2**). The pooled diagnostic performance of PI-RADS v2.1, for clinically significant(cs) PC shows sensitivity and specificity of 90% and 62%, respectively, for the whole gland (WG) assessment, and 0.90% and 0.67%, for the TZ. While PI-RADS v2.1 shows marginal improvement in sensitivity over PI-RADS v2, its specificity is reduced, increasing the likelihood of unnecessary targeted biopsies for PI-RADS 3 lesions [29].

Several advanced MRI pulse sequences, such as diffusion tensor imaging (DTI) [30], Blood oxygenation level dependent (BOLD) [31] and

Table 2. Limitations of PIRADS 2.1

Sr. No.	Limitations of PIRADS 2.1	Suggestive remarks
1	Lack of MRI based detection protocol for post-treatment monitoring of suspected PC recurrence, PC progression during surveillance	Should be included in revised version
2	Lack of detection protocol to investigate the other parts of the body having possibility to be involved with PC	Should be included in revised version
3	Lack of consensus-based surveillance strategies for PC detection at early stage	Should be included in revised version
4	Lack of elucidated or prescribed optimal technical parameters	Should be included in revised version
5	May miss the clinically significant PC, could possibly affect patient outcome [27]	PIRADS 2.1 guidelines with higher precision could curtail the unnecessary biopsy [27]
6	Lack of assessment of the background [28]	Inclusion of description of factors affecting mpMRI based PC detection [28]
7	Lack of guidelines for incidental outcomes. e.g. lesions involving central zone (CZ) [28]	A rational approach would be applied the criteria for the zone of origin of the lesion [28]

arterial spin labelling (ASL) [32] have demonstrated potential in PC detection and stratification. Ongoing research are needed to optimize the combination of pulse sequences, with some advocating for the exclusion of DCE imaging to enhance patient safety, reduce imaging time, and minimize costs. Additionally, the integration of advanced image processing techniques, including computer-aided diagnosis (CAD), is pivotal in refining diagnostic protocols.

The PI-RADS steering committee actively encourages the continued development of innovative MRI methodologies for PC assessment and local staging. Future strategies extend beyond the current PI-RADS v2.1 framework, aiming to incorporate novel and advanced research tools [24] (**Table 3**).

Artificial intelligence (AI) has revolutionized disease detection by improving accuracy, efficiency, and diagnostic throughput. Machine Learning (ML), a subfield of AI, employs probabilistic and statistical tools to recognize patterns in large datasets, thereby facilitating informed decision-making [40-42]. CAD, which fuses imaging feature analysis with ML classification, has shown considerable promise in assisting radiologists by enhancing diagnostic accuracy while being cost-effective [43]. Furthermore, Deep learning (DL), a specialized subfield of ML, utilizes artificial neural network (ANN) to extract meaningful patterns from data. DL has demonstrated promising results across various computer vision tasks, including segmentation, classification and, object detection [44-46] (**Figure 1**).

Despite the growing body of literature on MRI and AI-based approaches for PC detection, existing studies lack a comprehensive and up-to-date review of the combined impact of DL and MRI methodologies on diagnostic performance. A thorough evaluation of recent advancements and findings in this field is essential to further refine PC detection and stratification strategies, ultimately improving clinical outcomes.

Methods and analysis

Search strategy and sources

The PubMed database query was conducted using the search terms; “prostate cancer” AND “magnetic resonance imaging” AND “deep learning”, focusing on articles indexed in Medline. To ensure relevance, only full text articles published between January 2019 to March 2023, were included. The systematic review followed the Preferred Reporting Items for Systematic Reviews and Meta-analysis (PRISMA) guidelines [47] with a PRISMA checklist provided in **Appendix 1**.

Inclusion criteria

Studies were included if they met the following criteria: 1. Original articles indexed in PubMed and Medline. 2. Published between January

Table 3. Potential tactics under consideration for MRI-based prostate cancer diagnosis

Sr. No.	Further promising prostate MRI methodologies [24]	Interpretations	Parameters	References
1	Diffusion Tensor Imaging (DTI)	Microstructural properties of prostatic tissue [30]	Fractional Anisotropy (FA), Mean Diffusivity (MD)	[30]
2	Blood Oxygenation Level Dependent (BOLD)	Identification and quantification of regional distribution of hypoxia [31]	Rate of relaxation (R_2*)	[31]
3	Arterial Spin Labelling (ASL)	Tissue perfusion measurement by using magnetically labelled arterial blood protons	Signal intensity, Contrast ratio (CR), Perfusion rate (f)	[32]
4	Magnetic Resonance Spectroscopic Imaging (MRSI)	Evaluation of extent and aggressiveness of primary and recurrent PC [33]	Chemical shift	[33]
5	Diffusion Kurtosis Imaging (DKI)	Investigation of diffusion of water molecule and detection of the lesion microstructure [34] Relies on non-gaussian diffusion of water in biological system [35]	Mean Kurtosis (MK), Mean diffusivity (MD), Fractional Anisotropy (FA), Axial Kurtosis (AK), Radial Kurtosis (RK)	[34, 35]
6	MR-PET	Modality with combination of anatomic, functional and metabolic information [36]	ADC, Standardized Uptake Value (SUV)	[36]
7	Ultra-small superparamagnetic iron oxide (USPIO) agents	USPIO agents imaged with MRI, Method for visualizing lymph node metastasis [37]	T2* relaxation	[37]
8	Multiple b values assessment of fractional ADC	Quantitative evaluation of prostate cancer risk stratification	ADC calculation on different b values	[38]
9	Intravoxel-incoherent motion (IVIM) DWI	Separation of perfusion and diffusion	Pure tissue diffusion coefficient (Ds), Pseudo diffusion coefficient (Df), Volume fraction of pseudo diffusion (fp)	[39]

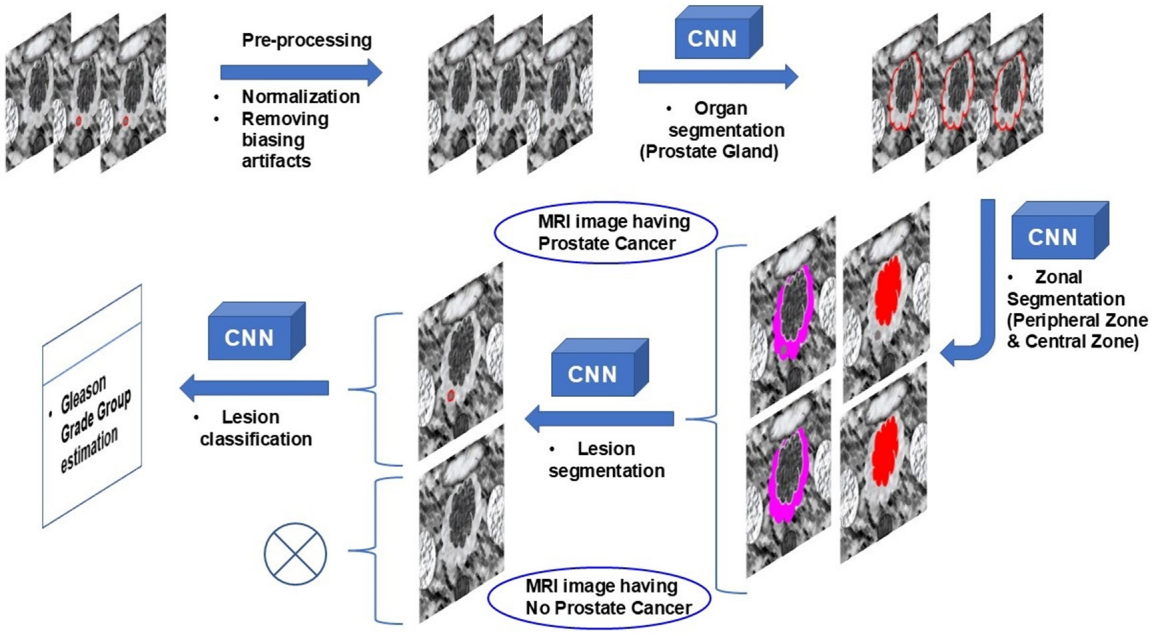

Figure 1. Schematic presentation of DL-based framework for detection and classification of prostate cancer.

2019 to March 2023. 3. Utilized DL with MRI for the PC detection and/or stratification. 4. MRI data acquired at a field strength of 3.0 Tesla. 5. Articles written in English. 6. Full text access availability.

Exclusion criteria

Studies were excluded if they met any of the following criteria: 1. Duplicate records. 2. Review articles, systematic reviews, meta-analysis, editorials, books, or other non-original research documents. 3. Use of non-relevant imaging techniques (e.g., CT, PET). 4. Focused on unrelated topics (e.g., segmentation, radiotherapy).

Study selection and data extraction

Records were retrieved from the database search, and duplicates were manually identified and removed by a single reviewer. Titles and abstracts of individual records were screened to ensure they met the inclusion criteria. The selected articles were then thoroughly reviewed and parameters relevant to the study design including patient cohort, DL methodology and performance matric were extracted and summarized (**Table 4**). Articles that were not written in English were excluded.

Quality of included articles

The assessment of the scientific quality of the included original articles was evaluated using the checklist for Artificial Intelligence in Medical Imaging [CLAIM] [48] (**Figure 2**; **Appendix 2**). The median agreement across 42 CLAIM items was 61.90% (IQR: 57.14-66.67, range 40.48-80.95%).

Additionally, the risk of bias was evaluated using the QUADAS-2 tool, which identified five studies [51, 62-64, 71] as being at high risk of bias (**Figures 3**, **4**).

Result

A total of 168 records were retrieved, of which 139 were excluded based on predefined exclusion criteria, leaving 29 articles for further analysis (**Figure 5**). The included studies were summarized with year-wise distribution (**Figure 6A**), patient distribution (**Figure 6B**), the proportion of prospective versus retrospective studies (**Figure 6C**), distribution of prospective and retrospective studies based on number of sites involved (**Figure 6D**).

A final set of 29 eligible articles included a total of 17,954 participants. Most of the studies were mono-centric (62.06%) and retrospective

Table 4. A detailed summary of included studies

Sr. No.	Objective	Retrospective/ Prospective	Multicentic study Yes/No	No of participants	Sequences used in DL workflow	DL network	Result	Year	References
1	PC detection, localization and segmentation	Retrospective	No	19	T2WI	Deep encoder-decoder 3D CNN	AUC: 0.995 Accuracy: 0.894 Recall: 0.928	2019	Akadi R et al. [49]
2	Comparative evaluation of DL based model to PI-RADS outcomes	Retrospective	No	312	T2, DWI, ADC	UNet	For PIRADS ≥4 vs. DL system (Probability threshold (≥0.33) Sensitivity=88% vs. 92% (P>0.99) Specificity=50% vs. 47% (P>0.99)	2019	Schelb P. et al. [50]
3	PC stratification	Retrospective	Yes	244	T2WI ADC	AlexNet	Accuracy: 86.92% Precison: 86.57%	2019	Yuan Y. et al [51]
4	PC detection, classification	Retrospective	No	204	T2WI, ADC, DCE	Model 1. VGG Model 2. Inception-Net	AUC model 1: 0.81 AUC model 2: 0.83	2019	Chen Q et al. [52]
5	Development of DL based model to detect csPC in low-risk PC cases	Prospective	No	292	T2WI, DWI and ADC	3D CNN	Average Sensitivity=82-92% Average Specificity=43-76% Average AUC=0.65 to 0.89	2020	Arif M. et al. [53]
6	PC detection and classification, Pulse sequence combination optimization for DL model	Retrospective	No	346	T2WI, DWI, ADC	MISN PZN TZN	ROC: 0.95	2020	Wang Y. et al. [54]
7	PC Detection	Retrospective	Yes	592	T2WI, DWI, ADC	CLaD	AUC: 0.81 Sensitivity: 83.23% Specificity: 59.18% Accuracy: 77.92%	2021	Hiremath A., et al. [55]
8	PC Detection	Retrospective	No	553	T2WI and DWI	Focal-Net	Differential sensitivity of Focal Net: 5.1%, 4.7% below the radiologist performance for CSPC and index lesions PC, respectively	2021	Cao R. et al. [56]
9	PC detection	Retrospective	No	424	T2WI, ADC	SPCNet	For csPC detection ROC_{RP}: 0.75 ROC_{BX}: 0.80	2021	Seetharaman A, et al. [57]
10	PC detection	Retrospective	No	100	T2WI, DWI, ADC	CNN	For csPC with PIRADS ≥4 $AUC_{radiologist}$: 0.84 $AUC_{DL\text{-}CAD}$: 0.88 P=0.010	2021	Winkel DJ et al. [58]
11	PC detection	Retrospective	No	259	T2WI, ADC	UNet	For PI-RADS ≥3 vs. Probability threshold d3: Sensitivity: 98% vs. 99% (P>0.99) Specificity: 17% vs. 24% (P>0.99) For PI-RADS ≥4 vs. Probability threshold d4, Sensitivity: 84% vs. 83% (P>0.99) Specificity: 58% vs. 55% (P>0.99)	2021	Schelb P et al. [59]

12	PC detection	Retrospective	No	414	DWI	CNN	Shallow CNN with random rotation $AUC_{validation}$: 88.93% AUC_{test}: 85.04%	2021	Hao R. et al. [60]
13	Transition zone PC detection	Retrospective	Yes	364	T2WI, ADC	UNet	Test set: using only ADC map as input, Sensitivity: 0.829 Precision: 0.617	2021	Wong T. et al. [61]
14	Assessment of image quality and diagnostic performance using DLR for suspected PC	Retrospective	No	60	DWI, ADC	Deep learning reconstruction (DLR)	For differentiation of malignant from benign: DWI_{3000} with DLR vs. without DLR: AUC: 0.89, 0.86 Sensitivity: 79%, 72% Specificity: 84%, 86% Accuracy: 82%, 79%	2022	Ueda T., et al. [62]
15	Establishment of DL based fully automated detection system for PC	Retrospective	Yes	525	T2WI, DWI, ADC	UNet and AH-Net	For test set sensitivity for UNet and AH-Net: 72.8% and 63.0%, respectively	2022	Mehralivand et al. [63]
16	DL based setup for PC detection and classification	Retrospective	Yes	1390	T2WI, DWI, ADC	3D U-Net	Sensitivity: 56.1%, PPV: 62.7%, PI-RADS classification accuracy: 30.8%	2022	Mehralivand et al. [64]
17	Localization, segmentation, GGG estimation of PC lesion	Prospective	Yes	565	T2WI, DWI, ADC and K^{trans}	Retina-UNet	For test set, lesion level, GGG ≥2; ProstateX data: AUC: 0.96 Sensitivity:1.0 Specificity: 0.79 IVO: AUC: 0.95 Sensitivity: 1.0 Specificity: 0.8	2022	Pellicer-Valero OJ et al. [65]
18	Accelerated PC MRI and detection	Retrospective	No	113	T2WI, DWI	Variational Network (VN) for image reconstruction	For PIRADS ≥3, Standard vs. VN-bpMRI performance: statistically non-significant. $Runtime_{std}$: 11.8 minutes $Runtime_{VN}$: 3.2 minutes	2022	Johnson PM. et al. [66]
19	PC detection and localization	Retrospective	Yes	2734	T2WI, ADC, DWI	DL-CAD	AUC: 0.85	2022	Hosseinzadeh M. et al. [67]
20	PC detection and localization	Retrospective	Yes	241	T2WI, ADC	Auto DL	for CG AUC: 0.94 With input T2 and ADC	2022	Zong W. et al. [68]

21	Identification and localization of indolent and aggressive PC	Retrospective	No	443	T2WI, ADC	CorrSigNIA	Segregated with and without PC with accuracy: 80%	2022	Bhattacharya I. et al. [12]
22	Detection and localization	Retrospective	No	390	T2WI, DWI, ADC	SPCNet	Model trained with digital pathologist labels: detection rate in Radical prostatectomy cohort: Aggressive lesion ROC-AUC: 0.91-0.94	2022	Bhattacharya I, et al. [69]
23	PC detection rate	Retrospective	No	170	T2WI, DWI and ADC	Quantib Prostate	For inexperienced reader Detection rate for csPC using bpMRI, Quantib and qADC: 0.16, 0.17 and 0.14 respectively For experienced reader Detection rate for csPC using bpMRI, Quantib, qADC and mpMRI: 0.18, 0.19, 0.16 and 0.20 respectively	2022	Cippolari S et al. 2022 [70]
24	PC detection	Retrospective	Yes	1861	T2, DWI, ADC	ResNet	The specificity of PIDL-CS for the detection of csPC was much higher than that of PI-RADS (P<0.05)	2023	Zhao L et al [15]
25	PC detection	Retrospective	No	354	T2WI, fDWI, zDWI	DL-CAD	Performance of DL-CAD model based on zDWI vs. fDWI b: AUC patient level: 0.89 versus 0.86; AUC lesion level: 0.86 versus 0.76	2023	Hu L. et al. [71]
26	PC detection and stratification	Retrospective	No	344	T2WI, DWI, ADC, Ktrans	CNN	AUC for T2-ADC-DWI: 0.90 AUC for T2-ADC-K^{trans}: 0.89	2023	Kim H et al. [72]
27	Development and evaluation of prostate cancer risk stratification tool; PRISK	Retrospective	Yes	1442	T2WI, DWI, ADC	Stacked ensemble learning algorithms	Overall accuracy PRISK vs. Biopsy Train: 85.1% vs. 88.7%, Internal test: 85.1% vs. 90.4% External test 90.4% vs. 94.2%	2023	Bao J et al. [73]
28	PC detection	Retrospective	Yes	1800	T2WI, DWI and ADC	UCNet	Improvement in generalization performance: Lesion classification: between 9.5-14.8%, Lesion segmentation: nearly 100%	2023	Rajagopal A et al. [74]
29	PC detection	Retrospective	Yes	1399	T2WI, DWI, ADC	UNet and TrumpeNet	AUC for external test: -for AI: 0.86 -for subspecialist: 0.86 (AI vs. subspecialist, P=0.88) -for Junior: 0.80 (P<0.05) -for general reader: 0.83 (P<0.05)	2023	Jiang KW et al. [75]

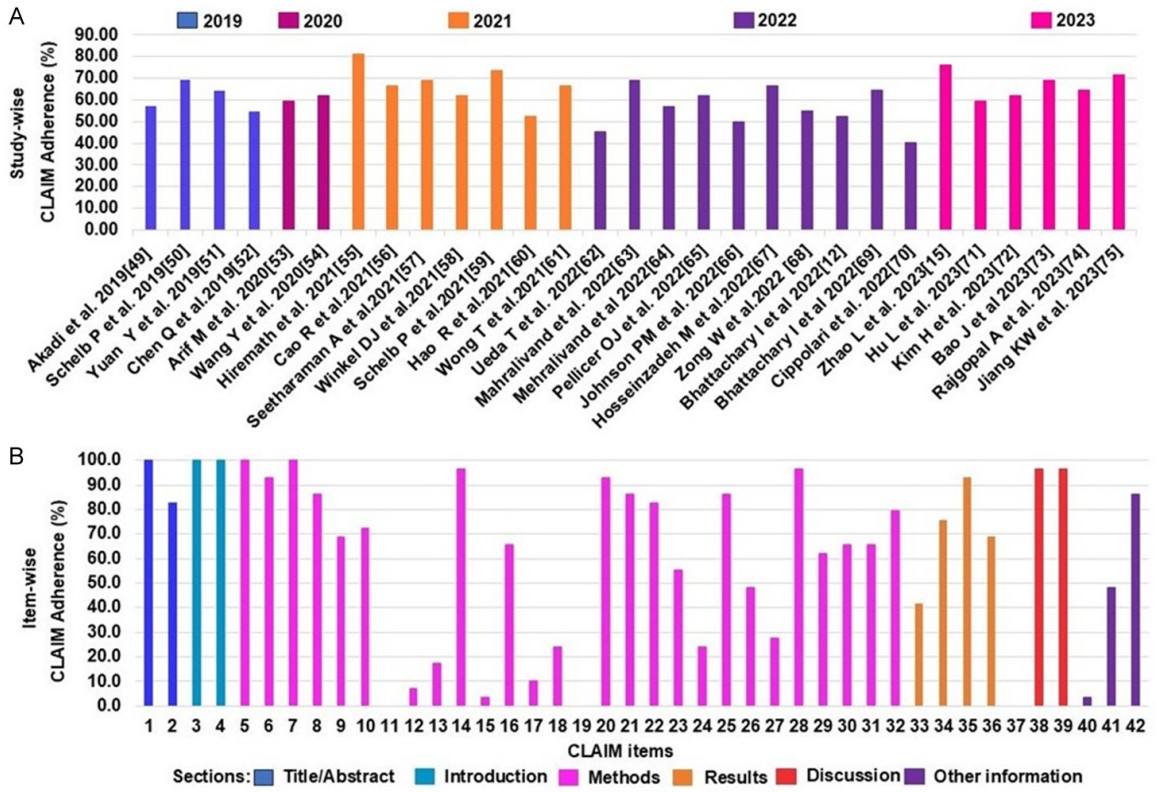

Figure 2. An outline of quality evaluation of included studies using the CLAIM checklist items, (A) Study-wise analysis, (B) Item-wise analysis across the studies.

(93.10%). Among the retrospective studies, 55.17% were monocentric, 37.93% multicentric, and 6.89% were prospective with monocentric involvement (**Figure 6**). The largest study included 1,861 participants, while the smallest had 19. Most of the studies utilized T2WI and/or ADC derived from DWI as inputs for the DL architecture. Four studies developed integrated models or monograms PC detection and stratification. Ten studies compared DL-based outcomes to those of experienced human radiologists, and ten studies utilized the ProstateX data set. Additionally, two studies applied DL to improve image quality in MRI protocols. A brief outline of the included studies is provided in **Table 4**, with key findings summarized below.

Tumor detection, localization and stratification

Different strategic approaches were applied, including the use of different CNN architectures, labeling techniques such as histopathology images labeling, radiological labeling, DL based improved image quality, to achieve the objectives.

Schelb P. et al. [50], performed a comparative study, examining lesion detection and segmentation for csPC, using DL-based setup trained with T2-weighted and diffusion MRI, compared to PI-RADS-based outcomes. For PI-RADS cut-off ≥4 on a per-patient basis, the sensitivity and specificity were 88% and 50% respectively. The study revealed a sensitivity of 96% and a specificity of 31% at a U-Net probability cut-off ≥0.22 whereas sensitivity was 92% and specificity 47% at a cut-off of ≥0.33 in the test set. The study concluded that the DL-based automated model performed similarly to PI-RADS when using T2WI and DWI for detection and segmentation of csPC [50].

Hiremath A. et al. [55], developed and assessed the potential of an integrated nomograms combining DL, PIRADS and clinical variables (PSA, prostate volume, lesion volume). The diagnostic performance of the model (ClaD) for detect-

Risk of bias domains
D1
D2
D3
D4
Overall
Study
Rajagopal A et al. 2023
Cao R et al 2021
Jiang KW et al. 2023
Zhao L et al. 2023
Hosseinzodeh M et al. 2022
Bhattacharya I. et al. 2022
Hu L et al. 2023
Bao J et al. 2023
Kim H et al. 2023
Hao R et al. 2021
Seetharaman A. et al. 2021
Akadi et al. 2019
Yuan Y et al. 2019
Ueda T et al. 2022
Zhong W et al. 2022
Arif. et al. 2020
Pellicer OJ et al. 2022
Wang Y et al. 2020
Chen Q et al. 2029
Schelb P et al. 2021
Winkel DJ et al. 2021
Schelb P et al. 2019
Johnson PM et al. 2022
Mahralivand et al. 2022
Hiremath et al. 2021
Mahralivand et al. 2022
Wong T et al. 2021
Indrani B et al. 2022
Cippolari et al. 2022
Domains:
D1: Patient selection.
D2: Index test.
D3: Reference standard.
D4: Flow & timing.
Judgement
High
Some concerns
Low

Figure 3. Traffic light plot for assessment of Risk of bias in included studies using QUADAS-2 tool. Plot was created using web based robvis tool.

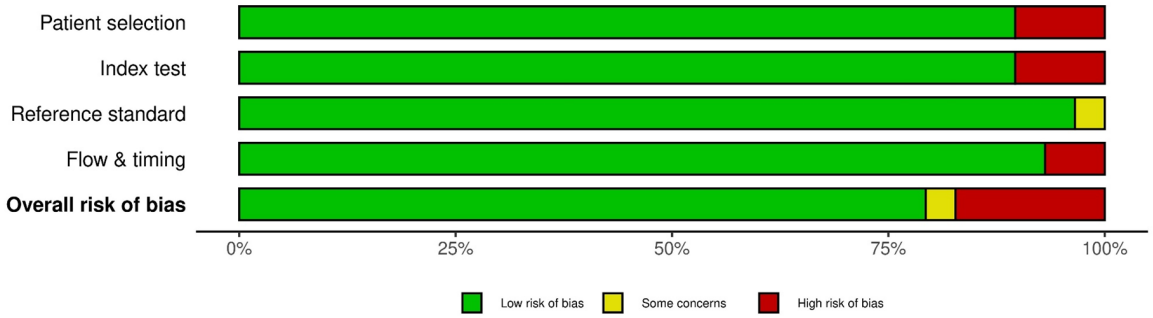

Figure 4. Summary plot for Risk of bias assessment in included studies using QUADAS-2 tool. Plot was created using web based robvis tool.

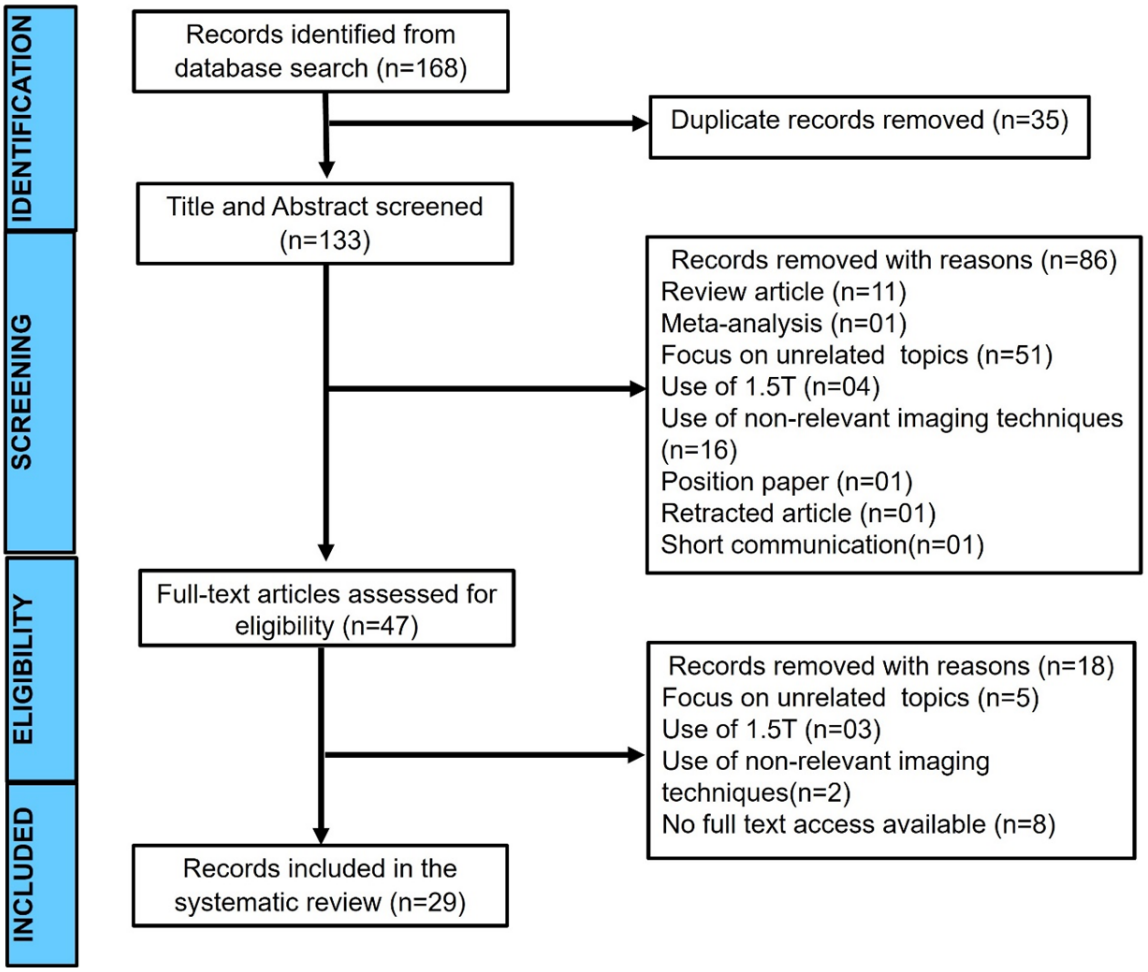

Figure 5. PRISMA flow diagram.

ing csPC revealed an accuracy of 77.92%, sensitivity of 83.23%, and specificity of 59.18% [55].

Cao R. et al. [56] compared the detection sensitivity of the DL algorithm Focal Net with human radiologists using whole mount histopa-

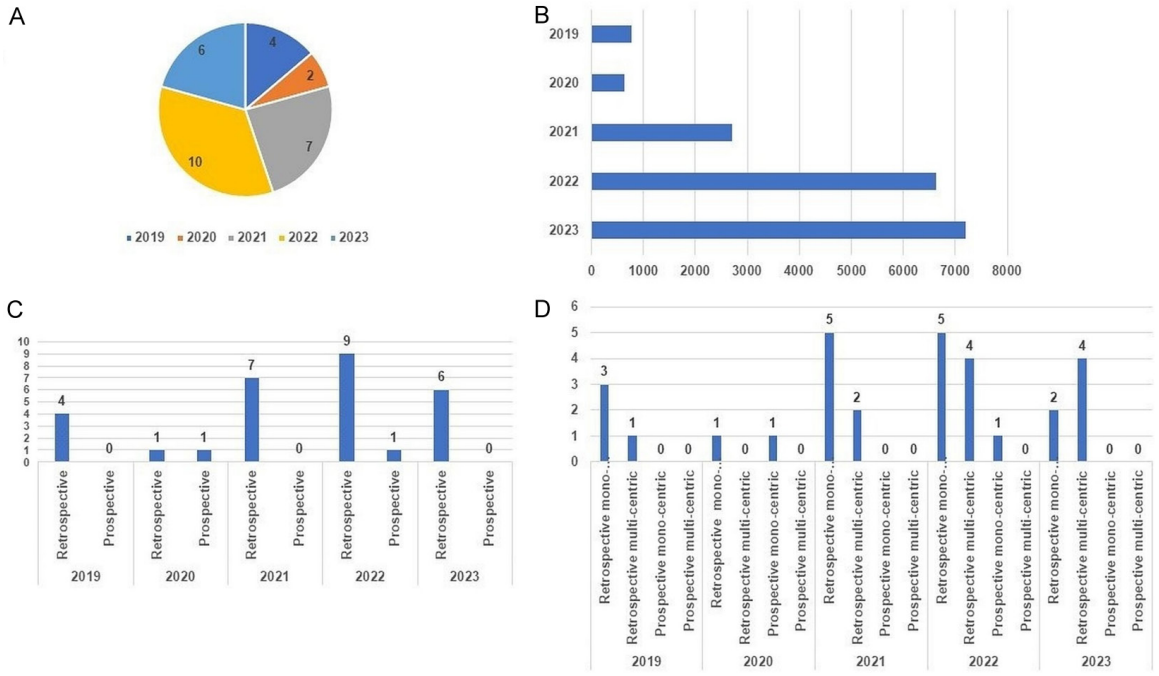

Figure 6. An overview of the included studies. A. Year wise distribution of number of included studies. B. Year wise patient distribution. C. The proportion of prospective versus retrospective studies. D. Distribution of prospective and retrospective studies based on number of sites involved.

thology (WMHP) as a reference. The T2WI and ADC were used as input images for Focal Net. The study included 553 patients, incorporating 427 in the developmental cohort and 126 in the evaluation cohorts. Bootstrap hypothesis test was performed to compare the performance of radiologists and Focal Net. The results showed a non-significant reduction in the differential detection sensitivity of Focal Net, which was 5.1% and 4.7% lower than that of the radiologists for clinically significant and index lesions, respectively (P=0.413 and P=0.282) [56].

Schelb P. et al. 2021 [59] assessed the performance of DL based model and compared it with clinical assessment in a single centered study involving 259 patients. The results revealed comparable for diagnostic performance; for PI-RADS ≥4 vs. UPT ≥d4, sensitivity was 84% vs. 83% (P>0.99) and specificity was 58% vs. 55% (P>0.99). The study also explored the model for simulated clinical deployment, focusing on automated evaluation of prostate MRI images. Significant improvement in positive predictive value were observed on both a per-patient and per-lesion basis, with concurrent detection and radiological assessment showing enhanced results [59].

Ueda T. et al. [62] applied deep learning reconstruction (DLR) to evaluate image quality and diagnostic performance in the differentiation of PC from benign areas of the prostate. In DWI with DLR, signal-to-noise ratios (SNRs) and contrast-to-noise ratios (CNRs) were observed significantly higher compared to imaging without DLR (P<0.001). However, ADC differences at each b value (i.e. b=1000, 3000, 5000), between malignant and benign areas did not show significant variation regardless of DLR. These findings suggest that DLR enhances the image quality of prostate DWI without affecting ADC quantification, presenting a promising method for improved lesion detection in PC [62].

Mehralivand S. et al. [63] utilized a dataset of bi parametric prostate MRI scans (n=525) were from two institutions to develop a fully automated DL-based PC detection system. MRI-visible lesions were contoured by experienced radiologists. Detection sensitivity for the UNet and AHNet models was reported as 72.8% and 63.0% respectively. A mean number of false positive lesions/patient using UNet and AH-Net was reported 1.90 and 1.40, respectively [63].

Mehralivand S. et al. [64] in a separate study, developed and evaluated a cascaded DL-based framework for detecting and classifying prostate lesions. The dataset included bi-parametric MRI scans (T2WI and DWI: ADC maps and high b-value DWI) from two institutions. A residual network architecture, U-Net, was trained on bi-parametric prostate images using PI-RADS. In the independent test set evaluation, the DL-based framework achieved a sensitivity of 56.1%, PPV of 62.7%, and FDR of 37.3% [64].

Bhattacharya I. et al. [12] developed a DL-based model, Correlated Signature Network for Indolent and Aggressive (CorrSigNIA), utilizing dual sources of characteristic features from registered MRI and whole mount histopathological imaging for PC detection and localization. The CorrSigNIA model achieved an accuracy of 80% in distinguishing men with and without PC. For lesion-level detection, the model demonstrated an ROC-AUC of 0.81±31 in a patient cohort that underwent both radical prostatectomy and biopsy [12].

Zhao L. et al. [15]. This multi-centric study investigated an integrated model (PIDL-CS), that constitutes a DL classification model between csPC vs. non-csPC (DL-CS) and PI-RADS outcomes. The model's outcomes were compared to PIRADS assessment alone. The findings revealed a higher AUC for csPC detection using the PIDSL-CS model compared to PIRADS assessment ($P<0.05$), except for one external validation set ($P>0.05$) [15]. PIDSL-CS model also exhibited significantly higher specificity for csPC detection than PI-RADS ($P<0.05$). This study highlights the potential of the PIDL-CS model as a specific tool for csPC detection, potentially reducing unnecessary biopsies [15].

Hu L. et al. [71] presented a DL-CAD model comparing the diagnostic performance of f-DWI and z-DWI, in differentiation of benign versus PC lesion group as well risk factors assessment affecting the diagnostic performance of PC assessment. DL-CAD model utilizing z-DWI showed significantly better overall accuracy compared that with f-DWI (z-DWI vs. f-DWI AUC patient level 0.89 vs. 0.86, AUC lesion level 0.86 vs. 0.76, $P<0.001$). The study identified contrast to noise ratio (CNR) of lesions as independent risk factor for false positives (OR= 1.12; $P<0.001$), whereas ADC, lesion diameter and rectal susceptibility artifacts identified as independent risk factors for both false negatives and false positives. These findings suggest improved diagnostic framework using MRI based DL-CAD models for PC assessment [71].

Bao J et al. [73] developed and evaluated the Prostate Imaging Stratification Risk (PRISK) model, which integrates a hybrid stacked-ensemble learning algorithm with high-throughput PC-MRI features and clinical indicators for PC risk stratification. The PRISK model was designed to classify benign cases (ISUP-GG 0) and ISUP-GG from grades 1 through 4/5. The findings demonstrated comparable performance between PRISK and invasive biopsy: training set (85.1% vs. 88.7%), internal test set (85.1% vs. 90.4%), and external validation set (90.4% vs. 94.2%), allowing for a grading error margin of ±1 ISUP-GG. The study highlighted PRISK as a promising non-invasive surrogate tool for assessing ISUP-GGs in PC [73].

Jiang K.W. et al. [75] developed and tested AI based model for PC diagnosis, utilizing a combination of an UNet and a TrumpetNet architectures for automatic prostate segmentation and lesion detection. The study compared the diagnostic performance of AI model with that of radiologist. In an external inpatient test, The AI model achieved a sensitivity of 86.9% and specificity of 65.9% at a probability score threshold of ≥45%. By comparison, junior readers demonstrated a sensitivity of 95.2% and specificity of 41.2%, subspecialist radiologist achieved 77.4% sensitivity and 87.1% specificity, and general radiologist showed 70.2% sensitivity and 84.7% specificity, all based on PIRADS score ≥3 [75].

Comparison of model performance to radiologists

In addition to evaluating the performance outcomes of DL based CNN architectures, a comparative assessment was conducted to determine their added value. This analysis included ten studies that compared DL-based models with human radiologists in detecting, localizing and stratifying lesions according to PI-RADS. Because of the inter-study variability and differing methodologies, the results could not be synthesized into a single conclusive finding. A summary of the comparative information from these studies is provided in **Table 5**.

Table 5. A summary of the comparative information of DL-based model versus radiologists

Sr. No.	Authors		Cut off	Sensitivity	CI range	Specificity	CI range	AUC	CI range
1	Schelb P et al. 2019 [50]	Radiologist	PIRADS ≥3	96 (25/26)	80-100	22 (8/36)	10-39		
			PIRADS ≥4	88 (23/26)	70-98	50 (18/36)	33-67		
		U-Net-Ensemble	UPT ≥0.22	96 (25/26)	80-100	31 (11/36)	16-48		
			UPT ≥0.33	92 (24/26)	75-99	47 (17/36)	30-65		
2	Cao R et al. 2021 [56]	Radiologist	Suspicion score ≥1 (CsPC lesion)	84.85					
		Focal Net	Suspicion score ≥1 (CsPC lesion)	83.9					
3	Schelb P et al. 2021 [59]	Radiologist	PIRADS ≥3	98 (106/108)	94-100	17 (25/151)	11-24		
			PIRADS ≥4	84 (91/108)	76-91	58 (88/151)	50-66		
		U-Net-Ensemble	UPT ≥d3	99 (107/108)	95-100	24 (36/151)	17-31		
			UPT ≥d4	83 (90/108)	75-90	55 (83/151)	47-63		
4	Hiremath et al. 2021 [55]	Radiologist	PIRADS (1-5)					AUC: 0.72	0.61-0.82
		Alex Net	DL-based imaging predictor					AUC: 0.76	0.71-0.81
			ClaD					AUC: 0.81	0.76-0.85
5	Seetharaman et al. 2021 [57]	Radiologist	Aggressive threshold 1%	0.72 (13/18)		1 (6/6)			
			Aggressive threshold 5%	0.71 (10/14)		1 (6/6)			
		DL	Aggressive threshold 1%	0.56 (10/18)		0.83 (5/6)			
			Aggressive threshold 5%	0.57 (8/14)		0.83 (5/6)			
6	Winkel DJ et al. 2021 [58]	Radiologist	PIRADS ≥3					AUC: 0.83	0.77-0.89
			PIRADS ≥4					AUC: 0.84	0.79-0.89
		DL	PIRADS ≥3					AUC: 0.86	0.79-0.92
			PIRADS ≥4					AUC: 0.88	0.83-0.94
7	Johnson PM et al. 2022 [66]	Radiologist	PIRADS ≥3	Reader 1: 0.40		0.55			
				Reader 2: 0.60		0.60			
				Reader 3: 0.60		0.58			
		DL	PIRADS ≥3	Reader 1: 0.60		0.64			
				Reader 2: 1.00		0.64			
				Reader 3: 0.60		0.55			
8	Hosseinzadeh M et al. 2022 [67]	Radiologist	PIRADS ≥4	91		77			
		DL	PIRADS ≥4					AUC: 0.85	0.79-0.91
9	Zhao L et al. 2023 [15]	Radiologist	PIRADS					AUC: 0.850	0.820-0.877
		DL	DL-CS-Res					AUC: 0.851	0.821-0.877
			PIDL-CS					AUC: 0.881	0.853-0.905
10	Jiang KW et al. 2023 [75]	Radiologist	csPC					AUC subspecialist: 0.86	0.80-0.90
		DL	TrumpetNet Thresold 0.45	86.9		65.9		AUC (AI): 0.86	0.81-0.91

CsPC: Clinically significant prostate cancer.

Table 6. Brief outline of the Integrated detection model/Nomogram/tool

Sr. No.	Nomogram/Tool/ DL based setup	Component	Annotations			ROC-AUC	References
			Radiologist	Pathologist	Clinical variables		
1	CLaD	PI-RADS score, DL based imaging predictors and clinical variables	No	Yes	Yes	0.81	Hiremath A., et al. [55]
2	SPCNet	CNN with annotated whole mount digital histopathology images	No	Yes	No	0.75 (RP cases) 0.80 (for biopsy patients)	Seetharaman A, et al. [57]
3	CorrSigNIA	CNN with dual source of groundtruths: MRI and digital histopathology images	Yes	Yes	No	0.81	Bhattacharya I. et al. [12]
4	PRISK	Integration of clinical indicators, high-throughput MRI features for PC with hybrid stacked-ensemble learning algorithms	No	No	Yes	For external test set: macro-AUC: 0.762	Bao J et al. [73]

Table 7. Brief outline of improvement in prostate MRI image quality and reduction in acquisition time using DL based tactics

Sr. No.	DL tactic	Value addition	Matric						References
			b value (sec/mm^2)	SNR with DLR	SNR without DLR	*p* value	CNR with DLR	CNR without DLR	*p* value	
1	Deep Learning Reconstruction (DLR)	Image quality	1000	38.7±0.6	17.8±0.6	<0.001	18.4±5.6	7.4±5.6	<0.001	Ueda T. et al. 2022. [62]
			3000	22.8±0.6	12.1±0.6	<0.001	16.4±6.6	7.0±3.9	<0.001	
			5000	15.9±0.6	9.5±0.6	<0.001	12.5±3.9	5.2±3.3	<0.001	
2	Variational Network (VN)	Acquisition time	With VN					Standard		Johnson PM et al. 2022 [66]
			3.2 minutes					11.8 minutes		

Abbreviations: SNR, signal-to-noise ratio; CNR, contrast-to-noise ratio.

Application of PROSTATEx grand challenge data

A total of 10 studies [51, 52, 54, 55, 58, 63-65, 72, 75] utilizes the PROSTATEx datasets. A brief overview regarding the studies is given in **Table 4**.

Integrated detection model/Nomogram/tool

A total of four studies [12, 55, 57, 73] developed and evaluated the performance of DL based model for the PC detection, localization and stratification (**Table 6**).

Improvement in prostate MRI image quality/ reduction in acquisition time

Two studies evaluated DL based approaches to improve the image quality [62] and developed the method for reduced scan time [66] (**Table 7**).

Discussion

PC remains a significant global health concern, and its early detection and accurate diagnosis are crucial for optimizing patient outcomes. Current diagnostic methods, such as mpMRI, while valuable, are hindered by inter-reader variability and subjective interpretation. We propose that AI should not only supplement existing methodologies but actively transform diagnostic workflows by embedding automated, self-improving algorithms into routine clinical practice. This approach will help reduce reliance on radiologist expertise, standardize assessments, and ultimately improve the accuracy and efficiency of PC diagnosis.

Advancements in mpMRI and AI for prostate cancer

Improving diagnostic accuracy: Despite the widespread adoption of the PI-RADS, inconsis-

tencies persist in its clinical application. While PI-RADS v2.1 introduced refinements, it has not significantly improved diagnostic accuracy. The pooled diagnostic performance of PI-RADS v2.1 for csPC does not outperform the earlier v2, showing slight improvement in sensitivity but reduced specificity, resulting in higher rates of negative targeted biopsies for PI-RADS 3 lesions [29]. In addition to these concerns, PI-RADS 2.1 presents several limitations (**Table 2**). In our view, PI-RADS should evolve into an AI-assisted system where deep learning models continuously adapt to real-world clinical data. This approach enables data-driven lesion classification, reducing dependence on subjective expertise. Therefore, it is imperative to enhance PI-RADS v2.1 with targeted measures to address these challenges effectively.

Deep learning in mpMRI: AI-driven DL models offer transformative potential in overcoming current limitations in mpMRI for PC detection and stratification. The primary focus should be on practical integration within clinical workflows rather than simply demonstrating technical feasibility in single studies.

Reduction in acquisition time: One of the major challenges of mpMRI for prostate imaging is its long acquisition time, which delays clinical decision-making and increases the duration of patient exposure under the strong magnetic field. We believe the most logical solution lies in Variational Networks (VN), which can significantly shorten scan duration while preserving diagnostic quality. However, rather than solely focusing on vendor-specific optimizations, research should prioritize vendor-agnostic AI models to ensure broad clinical applicability [66].

Improved DWI image quality: Image quality is a key limiting factor in accurately assessing the region of interest (ROI) within the field of view (FOV). Enhancing image quality while preserving pathophysiological imaging features can improve diagnostic potential. DLR has been shown to enhance the quality of DWI without affecting ADC quantitation, thereby improving lesion detection [62]. Future AI applications should incorporate adaptive filtering mechanisms that dynamically adjust noise reduction based on lesion morphology.

Data augmentation: To enhance model performance with a limited dataset, data augmentation techniques are applied. The primary goal is to determine the most effective augmentation method in conjunction with the best performing CNN architecture. Due to the prostate's symmetrical morphology, random rotation has been identified as the most effective augmentation technique for prostate DWI using a narrow CNN architecture [60].

Enhanced detection and staging: Inclusion of diversified data, relevant features and appropriate CNN architecture/s in the training set of DL model are key strategies to enhance the performance. Advanced architectures, such as convolutional encoder-decoder models, have demonstrated high accuracy in tumor segmentation and diagnosis, with AUC scores as high as 0.995 [49].

Comparative performance: The rapid detection and reporting of PC require urgent attention. The integration of DL has opened promising avenues to address this challenge. Further developments are needed to enhance the diagnostic accuracy and develop high-throughput systems for clinical use. DL-based models have demonstrated significant potential, often outperforming radiologists in PC detection and stratification (**Table 5**).

Multifaceted DL applications: Selection of robust input variables for the development of DL-based detection models, nomograms, and applications remains a major challenge. Various DL-based models, such as CorrSigNIA, CLaD, SPCNet, and PRISK, have been designed using various inputs, including PI-RADS scores, clinical variables, DL-based imaging predictors and annotated histopathology images, leading to improve diagnostic performance [12, 55, 57, 73].

Accelerated detection rates: Timely reporting is crucial for rapid clinical decision-making and treatment planning. AI-based software like Quantib has shortened reporting times for prostate bi-parametric MRI (bp-MRI) [70].

Improved diagnostic accuracy: Inter-reader variability remains a significant challenge in prostate MRI assessment. Integrating assistive tools may play a crucial role in enhancing diag-

nostic performance. DL-based computer-aided diagnosis (DL-CAD) systems have improved diagnostic accuracy, reduced reporting times and minimized inter-reader variability [58].

Federated learning: To maintain the participant's data privacy is one of the major concerns in multi-centric studies. Federated Learning (FL) has gained momentum in the healthcare sector for its potential to enhance data privacy, security and efficiency. Inclusion of diversified data-set along with radiological and histopathological annotations to train the model are major approaches to enhance the detection potential. AI model utilizing FL have shown promise in multi-centric study, enabling cross-site data collaboration while preserving patient privacy [74]. However, further research is needed to address the practical complexities to establish model with absolute performance.

Challenges in detection of TZ-prostate cancer: Detection and stratification of PC in the transition zone (TZ-PC) remains a challenge. TZ-PC accounts for approximately 30% of all PC cases, and its similarity to benign prostatic hyperplasia (BPH) on MRI often causes ambiguity in visual assessment. However, DL-based models have shown promising results in TZ-PC detection, achieving sensitivity and precision scores of 0.829 and 0.617, respectively, using only ADC as input [61]. We argue that a multi-parametric AI-driven approach, incorporating T2-weighted imaging, radiomics-based texture analysis, and AI-guided contrast enhancement, is essential for improving TZ-PC differentiation. Additionally, adaptive AI models that learn from individual patient imaging histories could further refine detection strategies.

Addressing bias in multi-centric MRI studies: In multi-center and multi-vendor studies, biases may arise due to inconsistencies in acquisition parameters, participant populations, imaging protocols, and scanner calibrations. These variations can impact the detection of subtle image features, ultimately impacting the diagnostic performance of AI models. Factors such as CNR, rectal susceptibility artifacts, ADC, and lesion diameter have been identified as key contributors to false positive and false negative results in DL-CAD models [71].

Recommendations for future studies

To evaluate the DL model performance more comprehensively, a multi-center prospective study should be designed with the following considerations: 1. Inclusion of multi-ethnic participant group with large sample size. 2. Use of multi-vender MRI machines. 3. Application of image quality enhancement techniques. 4. Inclusion of labelled imaging features from heterogenous cohorts, including annotated histopathology images for validation. 5. Use of optimized CNN architectures and performance-enhancing techniques. 6. Proportionate training and external validation cohorts, as well as comparative assessment against PI-RADS.

Limitations

The present review highlights several limitations: 1. Many of the included studies are retrospective and single-centered, often lacking comprehensive demographic information, which may reduce the relevance of their findings for broader consensus and diverse applications. 2. Excluding studies that utilized 1.5T MRI for data acquisition may limit the overall scope and inclusivity of the findings. 3. Restricting the review to articles published in English could result in the omission of valuable data from studies in other languages. 4. The exclusion of articles due to a lack of full-text access may further constrain the review's ability to present a comprehensive perspective on the topic. These limitations underscore the need for broader and more inclusive methodologies in future reviews.

Conclusion

In our view, this study underscores the significant potential of integrating prostate mpMRI with DL applications for the detection and stratification of PC. Although many of the studies reviewed were retrospective and single-centered, and some included comparisons with human radiologists, the promising results suggest that this integration could revolutionize clinical workflows. We believe the integration of mpMRI and DL represents a promising prototype for creating a more efficient and refined diagnostic system. This approach has potential to deliver sensitive, specific, non-invasive, and rapid detection and grading of PC, ultimately

leading to a more robust and automated system that could serve as an alternative to invasive biopsy.

Acknowledgements

Financial support was provided by the Indian Council of Medical Research [5/3/8/46/ITR-F/2020 to D.K.], New Delhi, India.

Disclosure of conflict of interest

None.

Address correspondence to: Dr. Hira Lal, Department of Radiodiagnosis, Sanjay Gandhi Post Graduate Institute of Medical Sciences, Rae Bareli Road, Lucknow 226014, U.P., India. Tel: +918004904486; E-mail: hiralal2007@yahoo.co.in; Dr. Ashish Gupta, Centre of Biomedical Research, Sanjay Gandhi Post Graduate Institute of Medical Sciences Campus, Rae Bareli Road, Lucknow 226014, U.P., India. Tel: +915222495034; E-mail: ashishg24@yahoo.co.in

References

[1] Sung Y, Ferlay J, Siegel RL, Laversanne M, Soerjomataram I, Jemal A and Bray F. Global Cancer Statistics 2020: GLOBOCON estimates of incidence and mortality worldwide for 36 cancer in 185 countries. CA Cancer J Clin 2021; 71: 209-249.

[2] Siegel RL, Miller KD, Wagle NS and Jemal A. Cancer Statistics 2023. CA Cancer J Clin 2023; 73: 17-48.

[3] Sanda MG, Cadeddu JA, Kirkby E, Chen RC, Crispino T, Fontanarosa J, Freedland SJ, Greene K, Klotz LH, Makarov DV, Nelson JB, Rodrigues G, Sandler HM, Taplin ME and Treadwell JR. Clinically localized prostate cancer: AUA/ASTRO/SUO guideline. Part 1: risk stratification, shared decision making, and care options. J Urol 2018; 199: 683-690.

[4] Catalona WJ, Smith DS, Ratliff TL, Dodds KM, Coplen DE, Yuan JJ, Petros JA and Andriole GL. Measurement of prostate specific antigen in serum as a screening test for prostate cancer. N Engl J Med 1991; 324: 1156-1161.

[5] Harvey CJ, Pilcher J, Richenberg J, Patel U and Frauscher F. Application of transrectal ultrasound in prostate cancer. Brit J Radio 2012; 85: S3-S17.

[6] Siddiqui MM, Rais-Bahrami S, Turkbey B, George AK, Rothwax J, Shakir N, Okoro C, Raskolnikov D, Parnes HL, Linehan WM, Merino MJ, Simon RM, Choyke PL, Wood BJ and Pinto PA. Comparison of MR/ultrasound fusion-guided biopsy with ultrasound-guided biopsy for the diagnosis of prostate cancer. JAMA 2015; 313: 390-397.

[7] Moe A and Hayne D. Transrectal ultrasound biopsy of the prostate: does it still have a role in prostate cancer diagnosis? Transl Androl Urol 2020; 9: 3018-3024.

[8] Xu G, Li J, Xiang L, Yang B, Chen Y, Sun Y, Zhao B, Wu J, Sun L and Xu H. Transrectal ultrasound examination of the prostate cancer guided by fusion imaging of multiparametric MRI and TRUS: avoiding unnecessary mpMRI-guided targeted biopsy. Asian J Androl 2023; 25: 410-415.

[9] Gosselaar C, Kranse R, Roobol MJ, Roemeling S and Schroder FH. The inter-observer variability of digital rectal examination in a large randomized trial for the screening of prostate cancer. Prostate 2008; 68: 985-993.

[10] Smith DS and Catalona WJ. Inter-examiner variability of digital rectal examination in detection prostate cancer. Urology 1995; 45: 70-74.

[11] Lumbreras B, Parker LA, Caballero-Romeu JP, Gomez-Perez L, Puig-Garcia M, Lopez-Garrigos M, Garcia N and Hernandez-Aguado I. Variables associated with false-positive PSA results: a cohort study with real-world data. Cancers 2022; 15: 261.

[12] Bhattacharya I, Seetharaman A, Kunder C, Shao Wei, Chen LC, Soerensen SJC, Wang JB, Teslovich NC, Fan RE, Ghanouni P, Brooks JD, Sonn GA and Rusu M. Selective identification and localization of indolent and aggressive prostate cancer via CorrSigNIA: an MRI-pathology correlation and deep learning framework. Med Image Anal 2022; 75: 102288.

[13] Ahmed HU, Bosaily AES, Brown LC, Gabe R, Kaplan R, Parmar MK, Collaco-Moraes Y, Ward K, Hindley RG, Freeman A, Kirkham AP, Oldroyd R, Parker C and Emberton M; PROMIS study group. Diagnostic accuracy of multi-parametric MRI and TRUS biopsy in prostate cancer (PROMIS): a paired validating confirmatory study. Lancet 2017; 389: 815-22.

[14] Johnson DC, Raman SS, Mirak SA, Kwan L, Bajgiran AM, Hsu W, Maehara CK, Ahuja P, Fajena I, Pooli A, Salmasi A, Sisk A, Felker ER, Lu DSK and Reiter RE. Detection of individual prostate cancer foci via multiparametric magnetic resonance imaging. Eur Urol 2019; 75: 712-720.

[15] Zhao L, Bao J, Qino X, Jin P, Ji Y, Li Z, Zhang J, Su Y, Ji L, Shen J, Zhang Y, Niu L, Xie W, Hu C, Shen H, Wang X, Liu J and Tian J. Predicting clinically significant prostate cancer with a deep learning approach: a multi-centre retrospective study. Eur J Nucl Med Mol Imaging 2023; 50: 727-741.

[16] Smith CP, Harmon SA, Barrett T, Bittencourt LK, Law YM, Shebel H, An JY, Czarniecki M, Mehralivand S, Coskun M, Wood BJ, Pinto PA, Shih JH, Choyke PL and Turkbey B. Intra and inter-reader reproducibility of PI-RADSv2: a multi-reader study. J Magn Reson Imaging 2019; 49: 1694-1703.

[17] Naji L, Randhawa H, Sohani Z, Dennis B, Lautenbach D, Kavanagh O, Bawor M, Banfield L and Profetto J. Digital rectal examination for prostate cancer screening in primary care: a systematic review and metanalysis. Ann Fam Med 2018; 16: 149-154.

[18] Merriel SWD, Pocock L, Gilbert E, Creavin S, Walter FM, Spencer A and Hamilton W. Systematic review and meta-analysis of the diagnostic accuracy of prostate-specific antigen (PSA) for the detection of prostate cancer in symptomatic patients. BMC Med 2022; 20: 54.

[19] Weinreb JC, Barentsz JO, Choyke PL, Cornud F, Haider MA, Macura KJ, Margolis D, Schnall MD, Shtern F, Tempany CM, Thoeny HC and Verma S. PI-RADS prostate imaging-reporting and data system: 2015, version 2. Eur Urol 2016; 69: 16-40.

[20] Kasivisvanathan V, Rannikko AS, Borghi M, Penebianco V, Mynderse LA, Vaarala MH, Briganti A, Budaus L, Hellawell G, Hindley RG, Roobol MJ, Eggener S, Ghei M, Villers A, Bladou F, Villeirs GM, Jaspal V, Boxler S, Robert G, Singh PB, Venderink W, Hadaschik BA, Ruffion A, Hu JC, Margolis D, Crouzet S, Klotz L, Taneja SS, Pinto P, Gill I, Allen C, Francesco G, Freeman A, Morris S, Punwani S, Williams NR, Brew-Graves C, Deeks J, Takwoingi Y, Emberton M and Moore CM; PRECISION Study Group Collaborators. MRI-targeted or standard biopsy for prostate-cancer diagnosis. N Eng J Med 2018; 378: 1767-1777.

[21] Tan CH, Wei W, Johnson V and Kundra V. Diffusion weighted magnetic resonance imaging in prostate cancer: metanalysis. AJR Am J Roentgenol 2012; 199: 822-829.

[22] Barentsz JO, Richenberg J, Clements R, Choyke P, Verma S, Villeirs G, Rouviere O, Logager V and Futterer JJ; European Society of Urogenital Radiology. ESUR prostate MR guidelines 2012. Eur Radiol 2012; 22: 746-57.

[23] Turkbey B, Rosenkrantz AB, Haider MA, Padhani AR, Villeirs G, Macura KJ, Tempany CM, Choyke PL, Cornud F, Margolis DJ, Thoeny HC, Verma S, Barentsz J and Weinreb JC. Prostate imaging reporting and data system 2.1: 2019 update of prostate imaging reporting and data system version 2. Eur Radiol 2019; 76: 340-351.

[24] Prostate Imaging Reporting and Data System (PIRADS) version 2.1. ACR-ESUR AdMe Tech 2019.

[25] Giganti F, Kasivisvanathan V, Kirkham A, Punwani S, Emberton M, Moore CM and Allen C. Prostate MRI quality: a critical review of the last 5 years and the role of the PI-QUAL score. Br J Radiol 2022; 95: 20210415.

[26] Scott R, Misser SK, Cioni D and Neri E. PIRADS v2.1: what has changed and how to report. SA J Radiol 2021; 25: 2062.

[27] Hotker AM, Bluthgen C, Rupp NJ, Schneider AF, Eberli D and Donati OF. Comparison of the PI-RADS 2.1 scoring system to PI-RADS 2.0: Impact on diagnostic accuracy and inter-reader agreement. PLoS One 2020; 15: e0239975.

[28] Purysko AS, Baroni RH, Giganti F, Costa D, Renard-Penna R, Kim CK and Raman SS. PI-RADS version 2.1: a critical review, from the AJR special series on radiology reporting and data system. AJR Am J Roentgenol 2021; 216: 20-32.

[29] Lee CH, Vellayappan B and Tan CH. Comparison of diagnostic performance and inter-reader agreement between PI-RADS v2.1 and PI-RADS v2: systematic review and meta-analysis. Br J Radiol 2022; 95: 20210509.

[30] Abouelkheir RT, Aboshamia YI and Taman SE. Diagnostic utility of three Tesla diffusion tensor imaging in prostate cancer: correlation with Gleason score values. Egypt J Radiol Nucl Med 2022; 53: 207.

[31] Kim Y, Park JJ and Kim CK. Blood oxygenation level-dependent MRI at 3T for differentiating prostate cancer from benign tissue: a preliminary experience. Br J Radiol 2022; 95: 20210461.

[32] Boschheidgen M, Schimmoller L, Kasprowski L, Abrar D, Arsov C, Albers P, Antoch G, Wittsack HJ and Ullrich T. Arterial spin labelling as a gadolinium-free alternative in the detection of prostate cancer. Magn Reson Imaging 2021; 80: 33-38.

[33] Verma S, Rajesh A, Futterer JJ, Turkbey B, Scheenen TWJ, Pang Y, Choyke PL and Kurhanewicz J. Prostate MRI and 3D MR spectroscopy: how we do it. AJR Am J Roentgenol 2010; 194: 1414-1426.

[34] Yao W, Zheng J, Han C, Lu P, Mao L, Liu J, Wang GC, Zou S, Li L and Xu Y. Integration of quantitative diffusion kurtosis imaging and prostate specific antigen in differential diagnosis of prostate cancer. Medicine (Baltimore) 2021; 100: e27144.

[35] Steven AJ, Zhuo J and Melhem ER. Diffusion kurtosis imaging: an emerging technique for evaluating the microstructure environment of the brain. AJR Am J Roentgenol 2014; 202: W26-W33.

[36] Evangelista L, Zattoni F, Cassarino G, Artioli P, Cecchin D, Moro FD and Zucchetta. PET/MRI in prostate cancer: a systematic review and meta-analysis. Eur J Nucl Med Imaging 2021; 48: 859-873.

[37] Czarniecki M, Pesapane F, Wood BJ, Choyke PL and Turkbey B. Ultra-small superparamagnetic iron oxide contrast agents for lymph node staging of high-risk prostate cancer. Transl Androl Urol 2018; 7 Suppl 4: S453-S461.
[38] Rogers HJ, Singh S, Barnes A, Obuchowski NA, Margolis DJ, Malyarenko DI, Chenevert TL, Shukla-Dave A, Boss MA and Punwani S. Test-retest repeatability of ADC in prostate using the multi-b value VERDICT acquisition. Eur J Radiol 2023; 162: 110782.
[39] Chen Z, Xue Y, Zhang Z, Li W, Wen M, Zhao Y, Li J, Weng Z and Ye Q. The performance of intravoxel-incoherent motion diffusion-weighted imaging derived hypoxia for the risk stratification of prostate cancer in peripheral zone. Eur J Radiol 2020; 125: 108865.
[40] Nasrabadi NM. Pattern recognition and machine learning. J Elec Imag 2007; 16: 049901.
[41] Goldberg DE and Holland JH. Genetic algorithms and machine learning. Machine Learning 1988; 3: 95-99.
[42] Michalski RS, Carbonell JG and Mitchell TM. Machine learning: an artificial intelligence approach. Springer Science & Business Media 2013.
[43] Yoo S, Gujrathi I, Haider MA and Khalvati F. Prostate cancer detection using deep convolutional neural networks. Sci Rep 2019; 9: 19518.
[44] Krizhevsky A, Sutskever I and Hinton GE. Image net classification with deep convolutional neural networks. In Advanc Neur Infor Process Sys 2012; 1097-1105.
[45] Long J, Shelhamer E and Darrell T. Fully convolutional networks for sematic segmentation. IEEE Trans Pattern Anal Mach Intell 2015; 3431-3440.
[46] He K, Zhang X, Ren S and Sun J. Deep residual learning foe image recognition. IEEE Trans Pattern Anal Mach Intell 2016; 770-778.
[47] Page MJ, McKenzie JE, Bossuyt PM, Boutron I, Hoffmann TC, Mulrow CD, Shamseer L, Tetzlaff JM, Akl EA, Brennan SE, Chou R, Glanville J, Grimshaw JM, Hrobjartsson A, Lalu MM, Li T, Loder EW, Mayo-Wilson E, McDonald S, McGuinness LA, Stewart LA, Thomas J, Tricco AC, Welch VA, Whiting P and Moher D. The PRISMA 2020 statement: an updated guideline for reporting systematic review. Int J Surg 2021; 88: 10590.
[48] Mongan J, Moy L and Kahn CE Jr. Checklist for artificial intelligence in medical imaging (CLAIM): a guide for authors and reviewers. Radiol Artif Intell 2020; 2: e200029.
[49] Alkadi R, Taher F, El-Baz A and Werghi N. A deep learning-based approach for the detection and localization of prostate cancer in T2 magnetic resonance images. J Digit Imaging 2019; 32: 793-807.
[50] Schelb P, Kohl S, Radtke JP, Wiesenfarth M, Kickingereder P, Bickelhaupt S, Kuder TA, Stenzinger A, Hohenfellner M, Schlemmer H, Maier-Hein KH and Bonekamp D. Classification of cancer at prostate MRI: deep learning versus clinical PI-RADS assessment. Radiology 2019; 293: 607-617.
[51] Yuan Y, Qin W, Buyyounouski M, Ibragimov B, Hancock S, Han B and Xing L. Prostate cancer classification with multiparametric MRI transfer learning model. Med Phys 2019; 46: 756-765.
[52] Chen Q, Hu S, Long P, Lu F, Yujie S and Li Y. A transfer learning approach for malignant prostate lesion detection on multiparametric MRI. Technol Cancer Res Treat 2019; 18: 1533033819858363.
[53] Arif M, Schoots IG, Tovar JC, Bangma CH, Krestin GP, Roobol MJ, Niessen W and Veenland JF. Clinically significant prostate cancer detection and segmentation in low-risk patients using a convoluted neural network on multi-parametric MRI. Eur Radiol 2020; 30: 6582-6592.
[54] Wang Y and Wang M. Selecting proper combination of mpMRI sequences for prostate cancer classification using multi-input convolutional neural network. Phys Med 2020; 80: 92-100.
[55] Hiremath A, Shiradkar R, Fu P, Mahran A, Rastinehad, Tewari A, Tirumani SH, Purysko A, Ponsky L and Madabhushi A. An integrated nomogram combining deep learning, prostate imaging-reporting and data system (PI-RADS) scoring, and clinical variables for identification of clinically significant prostate cancer on biparametric MRI: a retrospective multicentre study. Lancet Digit Health 2021; 3: e445-e454.
[56] Cao R, Zhong X, Afsari S, Felker E, Suvannarerg V, Tubtawee T, Vangla S, Scalzo F, Raman S and Sung K. Performance of deep learning and genitourinary radiologist in detection of prostate cancer using 3-T multiparametric magnetic resonance imaging. J Magn Reson Imaging 2021; 54: 474-483.
[57] Seetharaman A, Bhattacharya I, Chen LC, Kunder CA, Shao W, Soerensen SJC, Wang JB, Teslovich NC, Fan RE, Ghanouni P, Brooks JD, Too KJ, Sonn GA and Rusu M. Automated detection of aggressive and indolent prostate cancer on magnetic resonance imaging. Med Phys 2021; 48: 2960-2972.
[58] Winkel DJ, Tong A, Lou B, Kamen A, Comaniciu D, Disselhorst JA, Rodriguez-Ruiz A, Huisman H, Szolar D, Shabunin I, Choi MH, Xing P, Penzkofer T, Grimm R, Busch HV and Boll DT. A novel deep learning based computer-aided diagnosis system improves the accuracy and efficiency of radiologists in reading biparametric magnetic resonance images of the prostate:

results of a multireader, multicase study. Invest Radiol 2021; 56: 605-613.
[59] Schelb P, Wang X, Radtke JP, Wiesenfarth M, Kickingereder P, Stenzinger A, Hohenfellner M, Schlemmer H, Maier-Hein KH and Bonekamp D. Simulated clinical deployment of fully automatic deep learning for clinical prostate MRI assessment. Eur Radiol 2021; 31: 302-313.
[60] Hao R, Namdar K, Liu L, Haider MA and Khalvati F. A comprehensive study of data augmentation strategies for prostate cancer detection in diffusion-weighted MRI using convolutional neural network. J Digit Imaging 2021; 34: 862-876.
[61] Wong T, Schieda N, Sathiadoss P, Haroon M, Abreu-Gomez J and Ukwatta E. Fully automated detection of prostate transition zone tumors on T2-weighted and apparent diffusion coefficient (ADC) map MR images using U-Net ensemble. Med Phys 2021; 48: 6889-6900.
[62] Ueda T, Ohno Y, Yamamoto K, Murayama K, Ikedo M, Yui M, Hanamatsu S, Tanaka Y, Obama Y, Ikeda H and Toyama H. Deep learning reconstruction of diffusion-weighted MRI improves image quality for prostatic imaging. Radiology 2022; 303: 373-381.
[63] Mahralivand S, Yang D, Harmon SA, Xu D, Xu Z, Roth H, Masoudi S, Sanford TH, Kesani D, Lay NS, Merino MJ, Wood BJ, Pinto PA, Choyke PL and Turkbey B. Deep learning based artificial intelligence for prostate cancer detection at biparametric MRI. Abdom Radiol (NY) 2022; 47: 1425-1434.
[64] Mehralivand S, Yang D, Harmon SA. Xu D, Xu Z, Roth H, Masoudi S, Sanford TH, Kesani D, Lay NS, Merino MJ, Wood BJ, Pinto PA, Choyke PL and Turkbey B. A cascaded deep learning-based artificial intelligence algorithm for automated lesion detection and classification on biparametric prostate magnetic resonance imaging. Acad Radiol 2022; 29: 1159-1168.
[65] Pellicer-Valero OJ, Marenco Jiménez JL, Gonzalez-Perez V, Casanova Ramón-Borja JL, Martín García I, Barrios Benito M, Pelechano Gómez P, Rubio-Briones J, Rupérez MJ and Martín-Guerrero JD. Deep learning for fully automatic detection, segmentation, and Gleason grade estimation of prostate cancer in multiparametric magnetic resonance images. Sci Rep 2022; 12: 2975.
[66] Johnson PM, Tong A, Donthireddy A, Melamud K, Petrocelli R, Smereka P, Qian K, Keerthivasan MB, Chandarana H and Knoll F. Deep learning reconstruction enables highly accelerated biparametric MR imaging of the prostate. J Magn Reson Imaging 2022; 56: 184-195.
[67] Hosseinzadeh M, Saha A, Brand P, Slootweg I, Rooij MD and Huisman H. Deep learning-assisted prostate cancer detection on bi-parametric MRI: minimum training data size requirements and effect of prior knowledge. Eur Radiol 2022; 32: 2224-2234.
[68] Zong W, Carver E, Zhu S, Schaff E, Chapman D, Lee J, Bagher-Ebadian H, Movsas B, Wen W, Alafif T and Zong X. Prostate cancer malignancy detection and localization from mpMRI using auto-deep learning as one step closer to clinical utilization. Sci Rep 2022; 12: 22430.
[69] Bhattacharya I, Lim DS, Aung HL, Liu X, Seetharaman A, Kunder CA, Shao W, Soerensen SJC, Fan RE, Ghanouni P, To'o KJ, Brooks JD, Sonn GA and Rusu M. Bridging the gap between prostate radiology and pathology through machine learning. Med Phys 2022; 49: 5160-5181.
[70] Cipollari S, Pecoraro M, Forookhi A, Laschena L, Bicchetti M, Messina E, Lucciola S, Catalano C and Panebianco V. Biparametric prostate MRI: impact of a deep learning-based software and of quantitative ADC values on the inter-reader agreement of the experienced and inexperienced readers. Radiol Med 2022; 127: 1245-1253.
[71] Hu L, Fu C, Song X, Grimm R, von Busch H, Benkert T, Kamen A, Lou B, Huisman H, Tong A, Penzkofer T, Choi MH, Shabunin I, Winkel D, Xing P, Szolar D, Coakley F, Shea S, Szurowska E, Guo JY, Li L, Li YH and Zhao JG. Automated deep-learning system in the assessment of MRI visible prostate cancer: comparison of advanced zoomed diffusion-weighted imaging and conventional techniques. Cancer Imaging 2023; 23: 6.
[72] Kim H, Margolis DJA, Nagar H and Sabuncu MR. Pulse sequence dependence of a simple and interpretable deep learning method for detection of clinically significant prostate cancer using multiparametric MRI. Acad Radiol 2023; 30: 966-970.
[73] Bao J, Hou Y, Qin L, Zhi R, Wang X, Shi H, Sun H, Hu C and Zhang Y. High throughput precision MRI assessment with integrated stack-ensemble deep learning can enhance the preoperative prediction of prostate cancer gleason grade. Br J Cancer 2023; 128: 1267-1277.
[74] Rajgopal A, Redekop E, Kemisetti A, Kulkarni R, Raman S, Sarma K, Magudia K, Arnold CW and Larson PEZ. Federated learning with research prototypes: application to multi-center MRI-based detection of prostate cancer with diverse histopathology. Acad Radiol 2023; 30: 644-657.
[75] Jiang KW, Song Y, Hou Y, Zhi R, Zhang J, Bao ML, Li H, Yan X, Xi W, Zhang CX, Yao YF, Yang G and Zhang YD. Performance of artificial intelligence-aided diagnosis system for clinically significant prostate cancer with mri: a diagnostic comparison study. J Magn Reson Imaging 2023; 57: 1352-1364.

Appendix 1. PRISMA 2020 abstract checklist

Section and Topic	Items	Checklist item
TITLE		
Title	1	Integration of magnetic resonance imaging and deep learning for prostate cancer detection: A systematic review
BACKGROUND		
Objective	2	To evaluate the overall impact of incorporating deep learning (DL) with magnetic resonance imaging (MRI) for improving diagnostic performance in the detection and stratification of prostate cancer (PC)
METHODS		
Eligibility criteria	3	Inclusion Criteria: 1. Original articles indexed in PubMed and Medline 2. Published between January 2019 to March 2023 3. Utilized DL with MRI for the PC detection and/or stratification 4. MRI data acquired at a field strength of 3.0 Tesla 5. Articles written in English 6. Full text access availability Exclusion Criteria: 1. Duplicate records 2. Review articles, systematic reviews, meta-analysis, editorials, books, or other non-original research documents 3. Use of non-relevant imaging techniques (e.g., CT, PET) 4. Focused on unrelated topics (e.g., segmentation, radiotherapy)
Information sources	4	PubMed
Risk of bias	5	To access the risk of bias with applicability of primary diagnostic accuracy of studies QUADAS 2 tool was applied. To access the scientific quality, adherence with the of the Checklist for Artificial Intelligence in Medical Imaging (CLAIM) guidelines were applied
Synthesis of Results	6	Descriptive statistics, presented in the form of tables, figures and graphs
RESULTS		
Included studies	7	29 articles included; 17,954 participants included
Synthesis of results	8	The median agreement to the 42 CLAIM checklist items across studies was 61.90% (IQR: 57.14-66.67, range: 40.48-80.95). Most studies utilized T2WI and/or ADC derived from DWI as input for evaluating the performance of DL-based architectures. Detection and stratification of PC in the transition zone was the least explored area
DISCUSSION		
Limitations of evidence	9	1. Many of the included studies are retrospective and single-centered, often lacking comprehensive demographic information, which may reduce the relevance of their findings for broader consensus and diverse applications. 2. Excluding studies that utilized 1.5T MRI for data acquisition may limit the overall scope and inclusivity of the findings. 3. Restricting the review to articles published in English could result in the omission of valuable data from studies in other languages. 4. The exclusion of articles due to a lack of full-text access may further constrain the review's ability to present a comprehensive perspective on the topic
Interpretation	10	Integration of MRI with DL demonstrated a promising prototype for rapid, sensitive, specific, and robust detection and grading. of PC. Advanced applications include enhancing the quality of DWI, developing advanced DL models, and designing innovative nomograms or diagnostic tools to improve clinical decision-making
OTHER		
Funding	11	Financial support was provided by the Indian Council of Medical Research, New Delhi, India, Award No. [5/3/8/46/ITR-F/2020 to D.K.]
Registration	12	None

Appendix 2. CLAIM adherence evaluation of the included studies

	1	2	3	4	5	6	7	8	9	10	11	12	13	14	15	16	17	18	19	20	21	22	23	24	25	26	27	28	29	30	31	32	33	34	35	36	37	38	39	40	41	42	Total
Akadi et al. 2019 [49]	1		1	1	1	1	1	1	1					1		1				1	1	1			1	1		1			1	1		1		1		1	1		1	1	24
Schelb P et al. 2019 [50]	1	1	1	1	1	1	1	1	1	1				1		1				1	1	1	1		1		1	1	1	1	1	1	1	1	1	1		1	1			29
Yuan Y et al. 2019 [51]	1	1	1	1	1	1	1	1	1					1		1				1	1	1	1	1	1	1		1	1	1	1			1	1	1		1	1				27
Chen Q et al. 2019 [52]	1	1	1	1	1	1	1	1	1	1				1								1		1	1	1	1	1				1			1	1		1	1			1	23
Arif M et al. 2020 [53]	1	1	1	1	1	1	1	1	1		1			1		1				1		1			1	1		1	1			1	1	1	1			1	1		1	1	25
Wang Y et al. 2020 [54]	1	1	1	1	1	1	1	1		1				1		1				1	1	1	1		1		1	1	1	1	1	1			1	1		1	1			1	26
Hiremath et al. 2021 [55]	1	1	1	1	1	1	1	1	1	1			1	1		1		1		1	1	1	1	1	1	1		1	1	1	1	1	1	1	1	1		1	1		1	1	34
Cao R et al. 2021 [56]	1	1	1	1	1	1	1	1	1	1			1	1		1				1	1	1						1	1	1	1	1	1	1	1	1		1	1			1	28
Seetharaman A et al. 2021 [57]	1	1	1	1	1	1	1	1	1	1			1	1	1	1				1	1	1			1	1		1		1	1	1		1	1			1	1		1	1	29
Winkel DJ et al. 2021 [58]	1	1	1	1	1	1	1	1	1	1				1		1		1		1	1	1	1					1	1	1	1			1	1			1	1			1	26
Schelb P et al. 2021 [59]	1	1	1	1	1	1	1	1	1	1				1		1				1	1	1	1		1	1	1	1	1	1	1		1	1	1	1		1	1		1	1	31
Hao R. et al. 2021 [60]	1		1	1	1	1	1	1		1				1		1				1	1				1	1		1	1		1	1		1	1			1				1	22
Wong T. et al. 2021 [61]	1	1	1	1	1	1	1	1	1	1										1	1	1	1		1	1	1	1	1	1		1		1	1	1		1	1		1	1	28
Ueda T., et al. 2022 [62]	1	1	1	1	1	1	1	1						1				1							1			1					1	1	1	1		1	1			1	19
Mehralivand et al. 2022 [63]	1	1	1	1	1	1	1	1	1	1				1		1				1	1	1		1	1	1		1	1	1		1		1	1	1		1	1		1	1	29
Mehralivand et al. 2022 [64]	1	1	1	1	1	1	1	1		1				1			1			1					1			1	1	1		1	1	1	1	1		1	1			1	24
Pellicer-Valero OJ et al. 2022 [65]	1		1	1	1	1	1		1	1			1	1		1				1	1	1	1		1		1	1		1	1	1			1			1	1		1	1	26
Johnson PM. et al. 2022 [66]	1	1	1	1	1		1							1						1	1	1			1			1		1	1	1		1	1	1		1	1			1	21
Hosseinzadeh M. et al. 2022 [67]	1	1	1	1	1		1	1		1				1		1				1	1	1	1		1	1		1	1	1	1	1	1	1	1	1		1	1			1	28
Zong W. et al. 2022 [68]	1		1	1	1	1	1		1	1		1		1						1	1	1	1	1	1			1			1	1			1				1		1	1	23
Bhattacharya I. et al. 2022 [12]	1		1	1	1	1	1	1	1					1		1				1	1	1			1	1		1			1	1			1			1	1			1	22
Bhattacharya I, et al. 2022 [69]	1	1	1	1	1	1	1	1	1	1				1		1				1	1	1			1	1		1		1		1		1	1	1		1	1		1	1	27
Cippolari et al. 2022 [70]	1	1	1	1	1	1	1	1						1				1		1	1		1										1			1	1			1		1	17
Zhao L et al. 2023 [15]	1	1	1	1	1	1	1	1	1	1		1		1		1	1	1		1	1	1	1		1			1	1	1	1	1	1	1	1	1		1	1			1	32
Hu L et al. 2023 [71]	1	1	1	1	1	1	1	1		1				1						1	1	1	1					1	1	1			1	1	1			1	1	1	1	1	25
Kim H et al. 2023 [72]	1	1	1	1	1	1	1	1	1	1				1						1	1	1		1	1		1	1	1		1	1			1	1		1	1		1		26
Bao J et al. 2023 [73]	1	1	1	1	1	1	1	1	1	1				1						1	1	1	1	1	1	1	1	1	1			1	1	1	1	1		1	1			1	29
Raj Gopal et al. 2023 [74]	1	1	1	1	1	1	1	1	1					1		1		1		1	1	1	1		1			1		1	1	1		1	1			1	1		1	1	27
Jiang KW et al. 2023 [75]	1	1	1	1	1	1	1	1		1			1	1		1	1	1		1	1		1		1			1	1	1	1	1	1	1	1	1		1	1		1		30